REPORT DOCUMENTATION PAGE

AFRL-SR-AR-TR-05-

0118

1. AGENCY USE ONLY *(Leave blank)*	2. REPORT DATE	3. REPORT TYPE AND DATES COVERED
		15 Dec 2000 - 30 Nov 2004 FINAL

4. TITLE AND SUBTITLE
Investigation of Structural and Electrical Defects in GaN/AiGaN Structures and Modfets

5. FUNDING NUMBERS
61102F
2305/BX

6. AUTHOR(S)
Dr Morkoc

7. PERFORMING ORGANIZATION NAME(S) AND ADDRESS(ES)
VIRGINIA COMMONWEALTH UNIVERSITY
327 WEST MAIN STREET
RICHMOND VA 23284-3031

8. PERFORMING ORGANIZATION REPORT NUMBER

9. SPONSORING/MONITORING AGENCY NAME(S) AND ADDRESS(ES)
AFOSR/NE
4015 WILSON BLVD
SUITE 713
ARLINGTON VA 22203

10. SPONSORING/MONITORING AGENCY REPORT NUMBER
F49620-01-1-0085

11. SUPPLEMENTARY NOTES

12a. DISTRIBUTION AVAILABILITY STATEMENT
DISTRIBUTION STATEMENT A: Unlimited

12b. DISTRIBUTION CODE

13. ABSTRACT *(Maximum 200 words)*

In this project, main goal was to focus on MODFET structures to understand the sources of improvements and the sources of degradations. In order to reach one of the objectives, the CaN templates grown by MOCVD was followed by c-beam evaporation ofTi layer. By the means of in-situ nitridation in hydrogen and ammonia envtronrnent inside the MOCVD system, this Ti layer was converted into an effective nano-network of TiN with high density of voids and nano-porous CaN islands. Those nano-porous CaN templates were used as a template for nano-LEO epitaxy for CaN growth.

It has recently been reported the growth of thick CaN and subsequent separation from sapphire substrate by a void-assisted separation (VAS) technique. which uttlizes a thin TtN porous network at the beginning of hydride vapor phase epitaxy (HVPE) growth.' lhey obtained a very low TD density of 5xlt/ cm~ for the 300-~tm CaN layer on the TiN interlayer, as was reported by HVPE growth earlier in such CaN templates without a TiN network. It is, therefore, interesting to determine the role of a TiN network on dislocation reduction in thinner CaN films. In this paper, we report the growth and characterization of CaN grown on in situ TiN porous network by MOCVD with reduced dislocation density and therefore improved optical and crystalline properties.

14. SUBJECT TERMS

15. NUMBER OF PAGES

16. PRICE CODE

17. SECURITY CLASSIFICATION OF REPORT	18. SECURITY CLASSIFICATION OF THIS PAGE	19. SECURITY CLASSIFICATION OF ABSTRACT	20. LIMITATION OF ABSTRACT
Unclassified	Unclassified	Unclassified	UL

Final **Report prepared for Dr. Witt/AFOSR Award FA49620-01-1-0085 by Hadis Morkoç**

Investigation of Structural and Electrical Defects in GaN/AlGaN Structures and MODFETs

Objectives:

MODFETs fabricated on GaN films show a number of deviations from the ideal structures. This work will focus on the most likely sources of improvements, and paths to understand the sources of degradation. The primary focus will be on MODFETs, but the results will be applicable to a broad range of nitride devices. Leakage associated with the gates of MODFETs is a primary limitation in device performance. Current leakage paths, and also persistent photoconductivity, drain current lag, and current collapse, are related to electrically active dislocations, surface interface states, and metal induced gap states (MIGS). We will improve device capabilities through several means: growth conditions (e.g. temperature, V/III ratio), growth method (e.g. nano-LEO, HVPE templates, etching and regrowth), and post-growth passivation.

Progress:

Defect reduction by titanium nitride nanonet

In this project, main goal was to focus on MODFET structures to understand the sources of improvements and the sources of degradations. In order to reach one of the objectives, the GaN templates grown by MOCVD was followed by e-beam evaporation of Ti layer. By the means of in-situ nitridation in hydrogen and ammonia environment inside the MOCVD system, this Ti layer was converted into an effective nano-network of TiN with high density of voids and nano-porous GaN islands. Those nano-porous GaN templates were used as a template for nano-LEO epitaxy for GaN growth.

It has recently been reported the growth of thick GaN and subsequent separation from sapphire substrate by a void-assisted separation (VAS) technique, which utilizes a thin TiN porous network at the beginning of hydride vapor phase epitaxy (HVPE) growth.[1] They obtained a very low TD density of $5x10^6$ cm^{-2} for the 300-μm GaN layer on the TiN interlayer, as was reported by HVPE growth earlier in such GaN templates without a TiN network.[2] It is, therefore, interesting to determine the role of a TiN network on dislocation reduction in thinner GaN films. In this paper, we report the growth and characterization of GaN grown on *in situ* TiN porous network by MOCVD with reduced dislocation density and therefore improved optical and crystalline properties.

For the TiN layer experiment, a 0.7 μm GaN grown on sapphire by MOCVD was used as templates. Ti films of 20 nm and 10 nm were e-beam evaporated on the GaN templates and then subjected to a thermal annealing process at 1000 °C for 60 minutes, for a fixed ratio of NH_3 to H_2 (1:3) gases inside the MOCVD chamber. GaN overgrowth was then made on these two templates at 1030 °C, with constant TMGa flow rate of 78 μmol/min and NH_3 flow rate of 7.6 l/min. For comparison, a control

GaN layer was grown on the same GaN template using identical growth conditions but without the TiN network. The GaN sample with 20 nm TiN layer was characterized using cross-sectional and plan-view transmission electron microscopy (TEM), together with the control sample. Table I summarized the growth conditions and characterization results for all the samples

Sample#	Control	T68	CVD43
TiN layer	--	20 nm	10 nm
GaN overgrowth thickness (μm)	5.2 μm	7.5 μm	7.5 μm
XRD (002) FWHM (arcmin.)	3.9	3.8	5.0
XRD (102) FWHM (arcmin.)	7.6	5.4	4.5
Time-resolved PL Data (At room temperature)	τ_1=0.302±0.004ns τ_2=0.701±0.012ns A_2/A_1=0.429	τ_1=0.304±0.004ns $\tau_2$0.740±0.010ns A_2/A_1=0.529	τ_1=0.242±0.004ns τ_2=1.211±0.014ns A_2/A_1=0.562

Table I. List of GaN layers grown on 20 nm and 10 nm TiN porous networks, as well as the control GaN layer without TiN. The XRD data and time-resolved PL data are summarized here

Both samples were characterized by scanning electron microscope (SEM), x-ray diffraction (XRD), and room temperature time-resolved photoluminescence (TRPL). SEM images show that the surface morphology of TiN covered template is strongly affected by annealing time, but to a lesser extent by different gas ratios and annealing temperatures. In the annealing process, microscopic windows were formed on the Ti layer due to desorption of the Ti layer at high temperatures, accompanied by nitridation of this discontiguous Ti layer into a TiN network. At the initial annealing stage, closed chains were formed on Ti film, with a feature size of ~2μm. A similar phenomenon was also reported.[3] We suggest that these small windows (chains) first appeared at grain boundaries of underlying GaN template at the initial stage of nitridation. The less impervious nature of GaN at the grain boundaries and a possible catalytic effect of Ti on GaN decomposition lead us to this suggestion. As the *in situ* annealing process progresses, new windows begin to form at the grain boundaries and consequently both the density and size of those windows increase with time. Figure 1(a) shows the SEM surface morphology of TiN porous network formed on the 20 nm Ti layer. The cross-sectional TEM micrograph for the GaN with the 20 nm TiN porous network is shown in Fig. 1(b). It can be seen that the GaN growth on the TiN porous network initiated from the microscopic windows of the discontiguous TiN network acting as GaN islands. This is followed by the growth of GaN emanating from the islands by lateral and vertical expansion leading to coalescence. It can be discerned that thin and flat surface voids are formed above the discontinuous TiN layer, due to the lateral overgrowth of GaN and the possible "antisurfactant effect" of TiN. Threading dislocations significantly decease at or above the TiN/GaN interface. At least two mechanisms can be suggested for dislocation reduction related to GaN growth on TiN porous network. First, most of the threading dislocations in the GaN template are effectively blocked by the TiN layer. Second, some threading dislocations penetrate through the TiN windows to the upper layer but serendipitously

change their propagation direction and extend laterally instead. In the near-dislocation-free region above TiN, some *c*-plane stacking faults are formed due to gliding and dissociation of dislocations into partials. Burger's vector permitting, additional dislocation reduction could occur through recombination and annihilation. Therefore, the propagation of dislocations is effectively suppressed near the TiN/GaN interface. For comparison, the control GaN layer grown without the TiN interlayer is shown in Fig. 1(c), which shows no observable dislocation reduction above the initial GaN template.

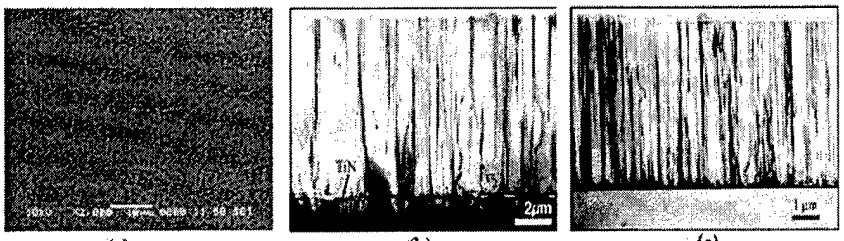

Figure 1. (a) SEM of TiN porous network (20 nm Ti layer), formed by in-situ annealing in NH_3/H_2 (1:3). Cross sectional TEM showing the effect of TiN porous network (with 20 nm Ti layer) on GaN dislocation reduction (b), and (c) GaN layer control w/o TiN.

A precise assessment of the amount of dislocation reduction can be made by counting directly the dislocations in the plan-view TEM micrographs. In Fig. 2(a), the plan-view image of the GaN control layer grown without TiN (13 μm in thickness) shows a high density of edge dislocation arrays (~$1.5 \times 10^9/cm^2$) as marked by "e", and a much lower density of isolated end-on screw dislocations (~$1.3 \times 10^8/cm^2$) as marked by 's". For the GaN grown with 20 nm TiN porous network (thickness of only 7.5 μm) shown in Fig. 2(b), the screw dislocation density is almost unchanged (~$1.4 \times 10^8/cm^2$), but the edge dislocations (~$0.9 \times 10^8/cm^2$) have decreased by at least an order of magnitude. These plan-view images suggest that the thin TiN porous network used is very effective in reducing edge dislocations. For screw dislocations, their numbers are already low (about 10% of the total dislocations) in MOCVD GaN, and the effect of TiN in reducing them is therefore less likely. High-resolution x-ray rocking curves (ω scan) show that the GaN samples grown on both 20 nm and 10 nm TiN porous networks have improved crystalline quality in terms of the full-width-at-half-maximum (FWHM) of the asymmetric ($10\underline{1}2$) diffraction peaks, as can be seen in Table I. Specifically, for the GaN samples with 20 nm and 10 nm TiN porous networks, FWHMs of ($10\underline{1}2$) peaks are 5.4 arcmin and 4.5 arcmin, respectively, as compared to 7.6 arcmin for the control sample. This is consistent with the TEM results in Fig. 2, which showed 10 × reduction in edge dislocations commonly associated with the asymmetric ($10\underline{1}2$) broadening which is sensitive to edge dislocations. The nearly unaffected symmetric (0002) FWHM is consistent with the TEM micrographs showing unchanged screw dislocation density. TRPL is a nondestructive and powerful technique commonly used to measure carrier lifetime, an important parameter related to material quality and device performance. Figure 2c shows the room temperature TRPL data for the GaN control sample (8 μm in thickness) with no TiN, and the GaN samples with 10 nm and 20 nm TiN porous

networks. The time-resolved signals were integrated over a 10 nm-wide spectral region around the peak PL energy (3.40 eV). The instrument-limited rise implies that the relaxation processes to cool the carriers from 3.81 eV excitation energy-defined states to the zero momentum excitonic band edge states are very fast. For both samples, the decaying part of the TRPL data is well described by a bi-exponential decay function: $A_1 \exp(-t/\tau_1) + A_2 \exp(-t/\tau_2)$. Table I tabulates the decay constants (τ_1 and τ_2) and the amplitude ratios (A_2/A_1) obtained from the fits.

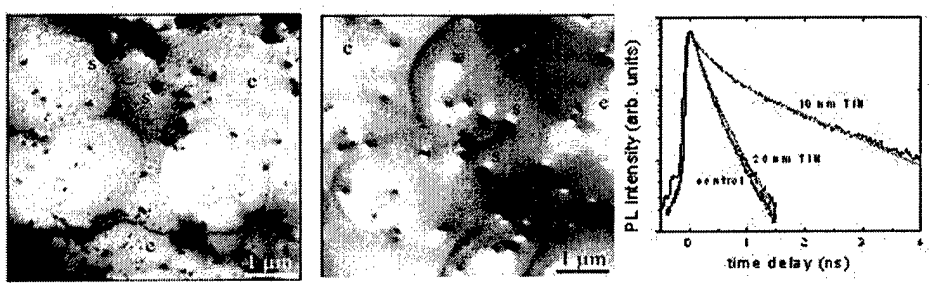

Figure 2. Plane-view TEM micrographs showing the edge and screw dislocations at the top of GaN surface, for (a) the control sample without TiN, and (b) the GaN with 20 nm TiN porous network, (c) time-resolved PL spectra showing bi-exponential decay of carrier lifetimes for GaN grown on TiN porous networks using 20 nm and 10 nm Ti layer, and without TiN (control).

The fast decay constant τ_1 most probably represents the effective non-radiative recombination at room temperature. The slow decaying component τ_2 is attributed to the radiative lifetime of the free exciton. Compared to the control sample, GaN sample with 10 nm TiN porous network shows almost a factor of 2 improvement in the carrier lifetime (τ_2). The decay times for the GaN sample with 20 nm TiN network is similar to that for the control sample. However, the relative magnitude of the slow decaying component to the fast decaying component (A_2/A_1) for both of the samples with TiN networks are improved compared to the control sample. This indicates that the nonradiative recombination is reduced by the inclusion of the TiN porous network. The considerable increase in the carrier lifetime (τ_2) for the 10 nm TiN sample rather than the 20 nm sample is somewhat puzzling since the XRD data for both of these samples show similar characteristics. However, one should keep in mind that in addition to the threading dislocations, the carrier lifetime is also sensitive to other types of defects such as point defects, the effects of which are not manifested by XRD in these films with relatively broad X-ray diffraction peaks.

Dislocation reduction by selective etch

The selectively etching of the dislocation defects and deposition of an overlayer will decrease the threading dislocation density, if the defective regions no longer provide a nucleation surface and growth takes place laterally from the etch pits. The selective etching of the defective regions was carried out by *ex-situ* with KOH. Some part of the samples grown by MOCVD technique was treated with molten KOH at 210 °C, one for 2 seconds and one for 30 seconds. Then overgrowth of 2 μm of GaN on the KOH etched and non-etched control GaN template was done at 1020 °C. Finally, a Mg-doped layer 200 nm thick was grown to form a *p-n* junction. Electrical

measurement, current versus voltage (I-V), was also performed and this measurement showed similar leakage currents for all of the treatments. The effect on the etched surface is seen in Fig. 3. KOH etching for 2 sec etches small pits in the surface. KOH etching for 30 sec opens up the pits to larger hexagonal shapes.

Structural and optical characterization did not reveal any significant differences in the material properties. X-ray diffraction full width at half maximum (FWHM) was 4.7-4.8 arcmin for the (002) line, with negligible difference between the etched and regrown, and non-etched and regrown layers. The (102) line was 6.9, 7.5, and 6.8 arcmin for the non-etched sample, the sample etched for 2 sec, and the sample etched for 30 sec, respectively. Photoluminescence spectra showed very similar characteristics for all samples, with no distinguishing differences as can be seen in Figure 4. The FWHM of the exciton peaks at 15K ranged from 4.6 to 7 meV.

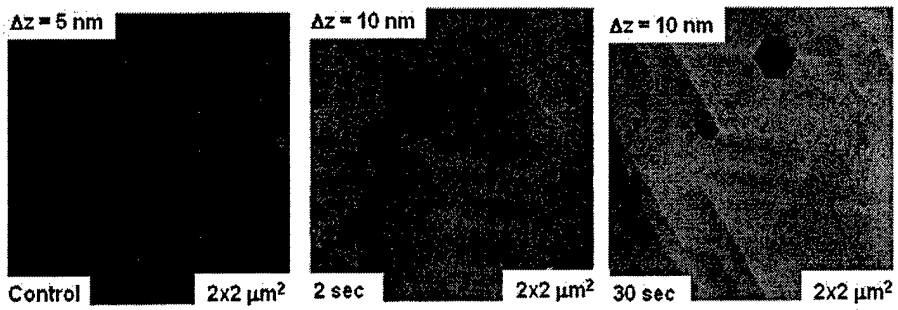

Figure 3. AFM images of the templates for regrowth of GaN by MOCVD. Etching for 2 seconds starts to open up pits. Longer KOH etching enlarges the pits and results in a layered structure.

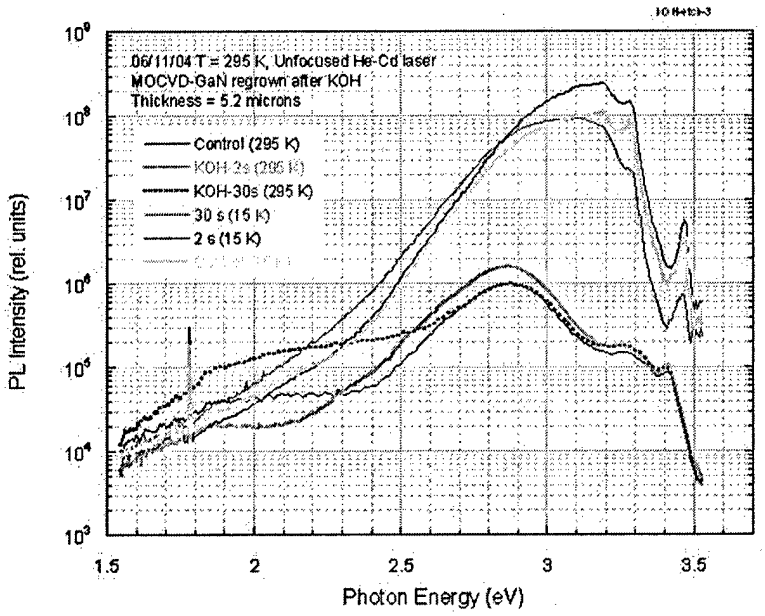

Figure 4. PL spectra of the templates for regrowth of GaN by MOCVD

Deep level transient spectroscopy (DLTS) was used to measure the defect concentration for each of the treatments, as well as the defect energies and capture cross sections. The DLTS setup is based on a SULA system, with added digitization of the transients for multi-exponential component fitting. Transients recorded at each temperature step were obtained by averaging ~2000 transients together, taking ~600 points at 0.1 msec sampling intervals. The filling pulse width was 10 msec. The temperature was varied in 4 K steps from 80 K to 700 K.

The rate window plot for the control sample, and the samples etched in KOH for 2 and 30 seconds in Figure 5(a) shows several traps. From this ratewindow plot, it appears that the 2 second etch in KOH was most effective at reducing the most prominent trap at 340 K. A comparison of the rate window plots for several scans from diodes processed identically revealed that the variation in the concentration of traps was nearly as large as those seen in Fig. 5(a). However, the trap concentration at 340 K was consistently lower for the material etched for 2 seconds compared to the control sample, or the sample etched for 30 seconds. Etching for 30 seconds produced some of the highest concentration traps at low temperature, below 200 K. None of the etching treatments eliminated any specific traps. The Arrhenius plot is given in Fig. 5(b), showing the energy for the electron and hole traps. Table I presents the characteristics of each trap. The hole trap at 75 meV has not been reported previously, nor has the observation of overlapping traps at 300-350 K with energies of 0.536 eV and 0.585 eV.

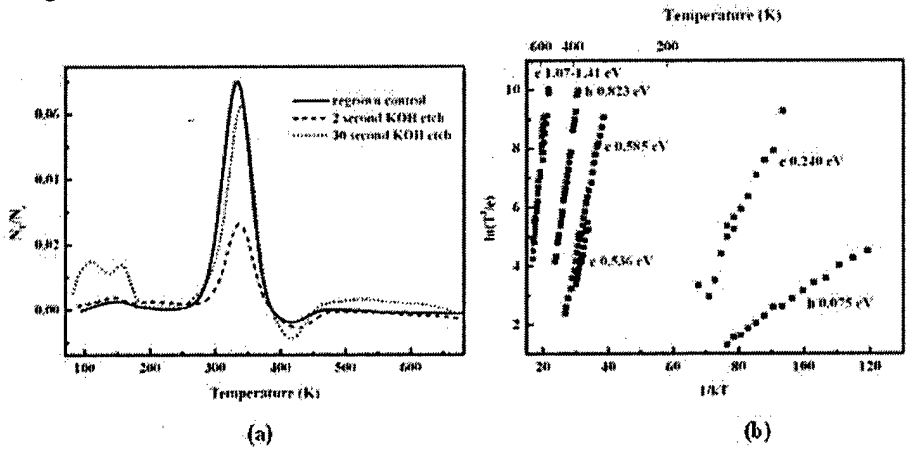

Figure 5. **(a)** DLTS ratewindow spectra for MOCVD grown GaN p-n junctions, comparing the non-etched regrown control sample, to GaN etched for 2 and 30 seconds in KOH prior to regrowth. The measurement conditions were: 3 V filling pulse, –1 V measurement bias, 10 msec filling pulse width. The ratewindow is 228/sec., **(b)** DLTS Arrhenius plot, traps at 0.24 eV and 0.585 eV are commonly seen in n-GaN grown by different methods. The hole trap at 75 meV, and the trap at 0.536 eV overlapping with the dominant trap at 0.585 eV have not been reported previously

The capture kinetics were also studied as a means to discriminate between point defects and linear defects, such as dislocations. Capacitance transient amplitudes from dislocations have been shown to have a logarithmic dependence on filling pulse width.[4] Increasing the filling pulse from 1 msec to 200 msec for the trap at 340 K resulted in a linear increase in amplitude when plotted versus the log of the filling pulse width, indicating that the trap is related to dislocations. The trap at 160 K showed a change in emission amplitude when varying the filling pulse width from 1 msec to 200 msec, but the response was complicated by the metastable nature of the trap, which is discussed next.

The concentration of traps measured at temperatures below room temperature depended on the conditions during cooling. The deep level spectra in Fig. 6 were collected under various conditions during cooling to 80 K, including 0 V, 150 mA (or micro A, 150 microamper in graph and caption) forward current, and –10 V. This shows that the configuration of defect structure depends on the presence of electrons, being electrically active when the traps are initially filled, similar to the study by Wu, et al. [5]. There is also an annealing effect as seen previously [6[6]], shown by the fact that the spectra taken after cooling with –10 V applied is higher than the spectra taken with 0 V cooling. As a result of this observation, all of the spectra in Fig. 2 were recorded after heating to 700 K, and with 150 mA applied during cooling to the starting temperature of 80 K.

Further measurements of the DLTS spectra showed that the difference between concentration of traps was as great between diodes on the same piece, as the difference between different treatments. This has also been seen by others (Fang, WSU) for other MOCVD samples.

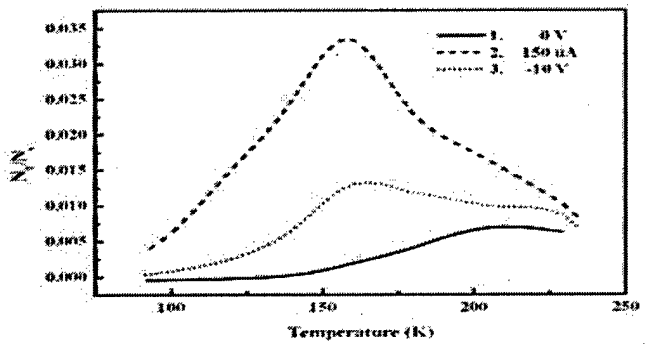

Figure 6. The concentration of deep levels at 160 K depended on the conditions during cooling, indicating a metastable configuration. Also, there is an annealing effect, since the spectra taken at –10 V should be lower than the spectra taken at 0 V. The order in which the spectra were taken is 1) 0 V, 2) 150 μA, 3) –10 V.

MBE growth kinetics for lateral epitaxy

RGA, RHEED, and AFM methods have been used to determine the desorption and diffusion energies of various species involved in the growth with RF nitrogen or ammonia, and molecules of N-Ga. The energy was determined as a function of crystal direction by exposing the face using etching and re-growth.

Gallium (Ga) surface desorption behavior was investigated using reflection high-energy electron diffraction (RHEED) during the GaN growth by plasma assisted

molecular beam epitaxy (PAMBE). It was found that the desorption of Ga atoms from the (0001) GaN surfaces under different III-V ratio deviates from the zeroth-order kinetics in that the desorption rate is independent of the coverage of adsorbed atoms. Although within a small temperature range under the same III/V ratio, the zeroth-order kinetics can be applied to find out the desorption energy approximately. The desorption energies are determined to be 2.78 eV for Ga from Ga droplets, 1.89 eV for Ga under Ga-rich growth conditions and 0.82 eV ~ 1.24 eV for Ga under stoichiometric growth conditions by monitor the intensity change of RHEED specular beam during the growth. The observation of the GaN surface morphology varying under different III-V ratio on porous templates matches the result that the Ga desorption energy dependents on the coverage, and III/V ratio dominates the growth mode.

Molecular beam epitaxy (MBE) is a promising method for fabrication of GaN-based heterostructure devices where high purity and precise control of layer thickness are required, since it has precise control of the beam fluxes and growth conditions.[7] Moreover, *in situ* characterization tools in MBE system allows access to parameters which shed light on the growth dynamics. So far, light-emitting diodes,[8] laser diodes,[9] UV photodetectors[10] and heterojunction field effect transistors[11] have been produced using GaN benefited from the capabilities of MBE. The comprehensive study of material and device properties have been carried out concerning surface structures, in particular for growth by plasma assisted molecular beam epitaxy (PAMBE).[12, 13] However, the intensive work on epitaxy of GaN for device applications still contrasts a relatively few studies on the physics of growth itself. Only recently, growth studies with MBE indicated that the growth mechanisms and the resulting surface structure of GaN thin films are crucially sensitive to the kinetics, i.e., Ga/N flux ratio and growth temperature. It is reported that the two-dimensional growth, which is desirable for device fabrication, is commonly attained under Ga-rich conditions or near Ga-rich conditions. This result suggests that the GaN growth front is stabilized by a metallic Ga adlayer.[14 - 17]

Ga desorption processes have been carried out previously by mass spectrometry[18, 19] and RHEED[16, 17, 22] techniques, however the results are not consistent. The wide range of activation energies reported for Ga desorption goes from 0.4 eV to 5.1 eV[17-19, 21-25], while the typically reported value for GaN decomposition is near 3.6 eV.[20] The Ga desorption energies in the absence of an active nitrogen flux were reported to be 2.05 eV, 3.7 eV, 3.1 eV and 2.2 eV from Al_2O_3 (0001)[21], 6H-SiC (0001)[22], GaAs[23], and GaN (0001) surfaces[18], respectively. The differences in the Ga desorption energies reported have been attributed to the Ga bond energy with different substrate atoms. Jones *et al.*[24] reported that the Ga desorption energy from GaN (0001) surfaces in the presence of NH_3 is 1.4 eV or 0.4 eV, depending of the substrate temperature, this suggest that the growth environment conditions modify the desorption energy. The effect on the desorption energy by the environmental conditions is confirmed by its dependence on the III/V ratio. [25] Furthermore,even the growth conditions can affect the desorption energy. However to our knowledge there has been no systematic study of Ga desorption energy as a function of the Ga surface coverage. In this work we analyze the desorption energy as a function of the Ga coverage.

In this study, reflection high-energy electron diffraction (RHEED) was used during GaN growth in PAMBE to investigate the Ga desorption behavior under different growth conditions. The results reveal a dependence of desorption energy of Ga from GaN surface on the Ga adlayer coverage which is determined by the III/V

ratio. The desorption energy was determined to be 2.78 eV under very Ga rich growth conditions with the Ga adlayer coverage close to 100%. This value is close to the activation energy for the evaporation of Ga from metallic Ga (2.81 eV[26]). With decreasing III/V ratio, the desorption energy decreased to 0.82 eV with coverage being about 10%. The different growth modes brought about by different III/V ratios are also investigated and reported.

The experiments were carried out using a plasma-assisted MBE system equipped with two conventional Ga effusion cells for the metallic species and a radio frequency (RF) plasma source for the nitrogen. (0001) GaN templates grown by metalorganic chemical vapor deposition (MOCVD) on sapphire were used as substrate since they have reproducibly smooth surfaces with atomically flat terraces. The GaN epilayers were grown on these substrates in the temperature range of 648 °C to 773°C. The *in situ* RHEED operated at 13.9 keV, and was directed along the [11-20] azimuth of the GaN (0001) surface with a fixed filament current at 1.4 A resulting in a fixed emission current. The intensity of RHEED specular beam was monitored when the growth was stable. The desorption energy was determined from the relationship between the intensity and substrate temperature for a given III/V ratio. To study the growth modes under different conditions, AFM surface topology measurements were carried out which allowed the investigation of the surface morphology of GaN which is re-grown on porous GaN templates under different III-V ratios while the substrate temperatures was kept at 700°C.

During the GaN growth in MBE, a certain fraction of active nitrogen flux Φ_N to gallium flux Φ_{Ga} arriving at the surface needs to be maintained for growth. When Ga atoms impinge on the GaN template surface, they are either incorporated into GaN epilayer with active nitrogen or adsorbed on the surface to form a Ga adlayer. On the other hand, some Ga atoms may re-evaporate from the Ga adlayer. The desorption process becomes significant particularly when the substrate temperature is higher than 550 °C.[17] The incorporation, adsorption and desorption processes reach a statistical equilibrium when GaN growth proceeds under steady condition, in which case the desorption rate can be expressed as[27]

$$k = \upsilon_0 \exp(-E_{des}/k_B T) \quad (1)$$

where υ_0 is the attempt frequency. At a GaN growth temperature by MBE (which is in the range of 650 °C ~ 780°C), the Ga adatoms does not condense into a reconstruction, but rather represent a liquid like film.[28] This disordered film causes an attenuation of the RHEED specular beam intensity.[29] As a result, the dependence of the desorption rate represented by the RHEED intensity vs substrate temperature provides the opportunity to study the desorption kinetics of Ga in real time. We interpret the relationship between the intensity of RHEED and the desorption energy as an exponential, given by:

$$I \sim \exp(-E_{des}/k_B T_s) \quad (2)$$

The Ga atoms desorbs from the surface at a substrate temperature T_s with the desorption energy E_{des}.

Figure 7 shows the typical trend of the variation of RHEED specular beam intensity during GaN growth at different substrate temperatures under the stoichiometric conditions. In this case, the Ga flux is slightly higher than that for nitrogen. The Ga cell temperature was kept constant at 1140 °C, and the pressure was 8×10^{-6} Torr. The substrate temperature was varied from 648 °C to 680 °C. Since this temperature range is small, it can be assumed that the coverage change of the Ga adlayer on GaN surface caused by increasing substrate temperature is negligible.

Therefore, the desorption energy can be treated as a constant and calculated by the zeroth-order desorption kinetics. The exponential relationship in **Figure 7** supports this assumption, and the desorption energy E_{des} = 0.82 eV is determined by using equation (2).

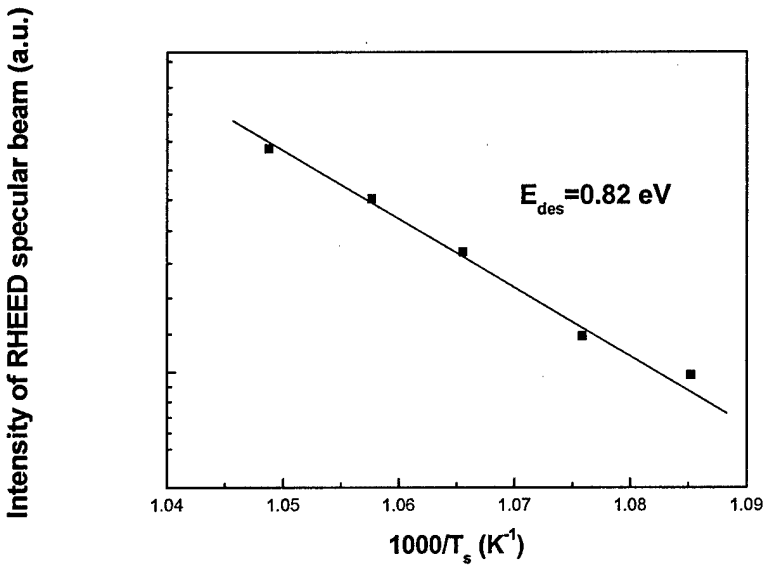

Fig. 7. The variation of the RHEED specular beam intensity during the GaN growth for substrate temperatures from 648 °C to 680 °C under stoichiometric growth condition. The Ga cell temperature is kept constant at 1140 °C, and the pressure is $8x10^{-6}$ Torr.

It is also found that the desorption energy changes under different growth conditions. Higher Ga desorption energies from GaN surface resulted for higher III/V ratios. Under stoichiometric conditions, the desorption energies are in the range of 0.82 to 1.24 eV, slightly increasing with the number of Ga atoms on the surface. Under Ga-rich conditions, the desorption energy is determined to be 1.89 eV for substrate temperatures in the range of 692 °C to 749 °C. On the other hand, the desorption energy is 2.78 eV in the absence of any active nitrogen flux. In this case, Ga atoms accumulate on the GaN surface without forming a GaN epilayer, and the coverage of Ga adlayer is approximately 100%.

Table 2 lists the results of Ga desorption energies for different III/V ratios on the GaN surface at different substrate temperatures. It is clear that the growth environment affects on the Ga desorption energy . This phenomenon can be explained by the dependence of desorption energy on the bond strength which is determined by the separation between atoms. A simple approach based on the Madelung Model[26] allows a first degree understanding of the relationship between the cohesive energy and the separation between atoms:

$$U(r_0) = -\frac{N\alpha q^2}{r_0}\left(1-\frac{\rho}{r_0}\right) \qquad (3)$$

Equation (3) shows the total energy of the crystal of 2N ions at their equilibrium separation r_0, while α is Madelung constant and the parameter ρ is of the order of $0.1r_0$. Using this approach, it is clear that the bond energy has a reciprocal relationship to the separation, r_0. Under the steady state condition of GaN growth, the equilibrium separation r_0 between Ga-Ga atoms depends on the growth conditions, and the average in-plane separation r between Ga-Ga atoms can be related to the Ga coverage C as follow:

$$C(r) \propto 1/r^2 \quad (4)$$

Ultimately, the relationship between the Ga desorption energies and surface coverage can be deduced.

Table 2. Summary Ga desorption energy for different Ga coverage on the GaN surface at different substrate temperatures iindicated in the "T_s range" row .

Ga density in Ga monolayers	→					
Growth condition	Stoichiometric regime			Ga-rich regime		Ga-droplet regime
E_{des} (eV)	0.82	0.94	1.24	1.59	1.89	2.78
T_s range (°C)	648~680	659~696	667~727	658~708	692~749	752~773

In our study, the Ga desorption energy was determined to be 2.78 eV under Ga very rich condition with a coverage about 100%. This result is very close to the cohesive energy of Ga (2.81eV[26]), defined as that energy required to remove a Ga atom from a Ga reservoir. Since this condition corresponds to a Ga-Ga separation of 2.7 Å[30, 31], the coverage of Ga under different growth conditions can be calculated based on these values. The results of such an exercise are listed in **Table 3.** The coverage is determined to be 45% under Ga-rich conditions when the desorption energy is 1.89 eV. Under the stoichiometric conditions most Ga atoms tend to form GaN epilayer, and only a few Ga atoms stick on the surface and the Ga monolayers coverage is low. The desorption energy is about 0.82 eV when the coverage decrease to about 10%.

Table 3. The desorption energies with different Ga-Ga separation and Ga coverage.

E_{des} (eV)	0.82	0.94	1.24	1.59	1.89	2.78
Ga-Ga Separation (Å)	9.2	8	6.1	4.8	4	2.7
Coverage (%)	8.6	11.4	19.6	31.6	45.6	100

Varying GaN surface morphology under different III-V ratio on porous templates at a temperature 700°C is consistent with the Ga desorption energy being dependent on the coverage. **Figure 8** shows a typical AFM image of GaN epilayers etched in molten KOH for 1 min, which are later used as templates for further growth. The pores on the template have a hexagonal shape of about 200nm in width and 50nm in depth. After a 2-hour re-growth of GaN by MBE on these templates, the surface

morphologies vary under different growth condition. Typical AFM images of GaN re-grown under stoichiometric conditions and Ga-rich condition are shown in **Figure 8 (2)** and **(3)**, respectively. Under stoichiometric conditions, hexagonal pits still appear on the surface with a depth of 50nm which is similar to that of the substrate. However, under Ga-rich condition, the surface of GaN is atomically smooth without pits.

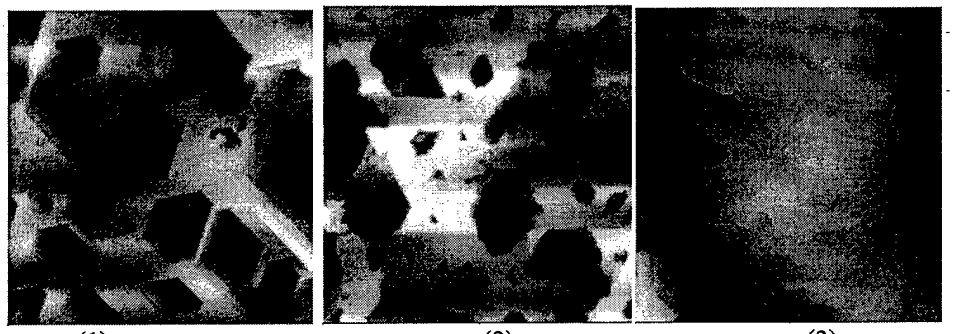

(1) (2) (3)

Fig. 8. The dependence of surface morphology of GaN for different III-V ratios during growth at 700 °C on KOH etched GaN templates. (1) the surface morphology of etched GaN template; (2) The surface morphologies of GaN grown for 2-hour under stoichiometric conditions; and (3) the same under Ga-rich condition.

Deleted: under

Deleted: growth GaN

This phenomenon indicates that the III/V ratio dominates the surface oriented processes which strongly affect the surface morphology. The desorption energy falls in the range of 0.82 - 2.78 eV with III/V ratio increasing, which ompares with the reported Ga diffusion energy, of about 1.45 eV,[32, 33] Under stoichiometric conditions, the diffusion energy is larger than the desorption energy. Therefore, a Ga atom prefers to incorporate into the GaN film with N at the arrival site or desorbs from the surface, instead of diffusing to a new site, and the growth has an isotropic nature. In contrast the diffusion energy is smaller than the desorption energy under Ga-rich conditions. Ga atoms are very mobile in this case and they prefer to move about on the surface to find new site with lower potential energy, such as the edge of a step or the bottom of a pit. As a result, the GaN growth mechanism follows the layer-by-layer growth mode with the pores being filled and the surface turning smooth as growth proceeds.

In summary we investigated the Ga desorption kinetics on GaN (0001) surfaces using reflection high energy electron diffraction during GaN growth. We found that the desorption energy of Ga depends on the Ga coverage which is determined by the III/V ratio. For a very high III/V ratio, the desorption energy is 2.78 eV with the coverage being about 100%, while the desorption energy is about 0.82 eV under the stoichiometric growth condition with the coverage being about 10%. The variation in the desorption energy with the III/V ratio may be attributed to the difference in the Ga-Ga separation in Ga adlayer. By controlling the III/V ratio, different growth modes of GaN in MBE growth can be obtained as a result of competition between the desorption and diffusion processes.

Metal/semiconductor interface and surface states

The effects of chemical passivation and etching on M/S interface and surface states were investigated. This study would allow devices with better performance characteristics such as lower surface leakage paths and metal/semiconductor interface states. For this purpose, three MOCVD grown GaN layers were chosen, one is for control, one for RIE and another for RIE followed by KOH. Figure 9 shows the AFM images of these samples. As can be seen, the RMS value for the RIE etched sample is increased almost three times compared the control sample. After RIE followed by KOH, the RMS value decreased to the lowest value compare to control sample. This is an indication that the RIE damage is removed as well the natural smoothening afforded by the relatively larger etching rates for prismatic planes. Figure 10 shows the I-V curves for different devices for each sample. The improvements have been observed by I-V and DLTS measurement, but ideality factor did not show much contact improvement. There is considerable activity in the GaN field indicating that perhaps that there is highly doped region on the surface of GaN which causes contribution from tunneling or thermionic field emission current both of which would have greater than unity ideality factor. The current study indicates that had this been due to some increased donor concentration near the surface emanating from the growth, that region would have been removed in the etch and that improved ideality factors would have resulted. What remains, of course, is the possibility of damage during fabrication which may cause the increase doping near the surface.

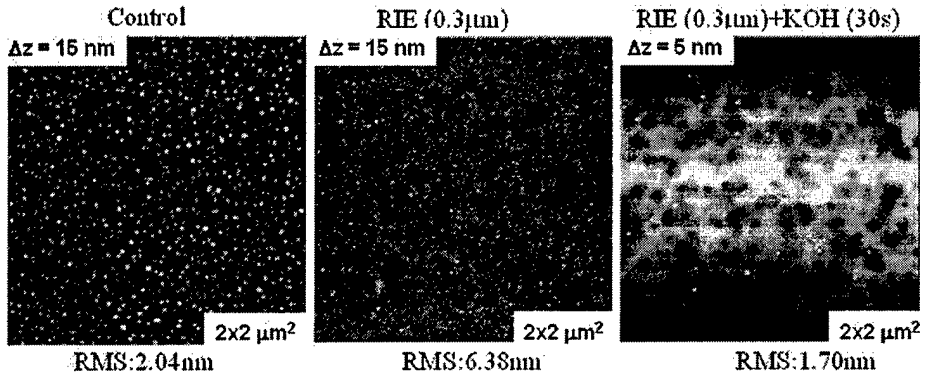

Figure 9. The AFM images of the MOCVD grown GaN for two different treated condition together with control sample.

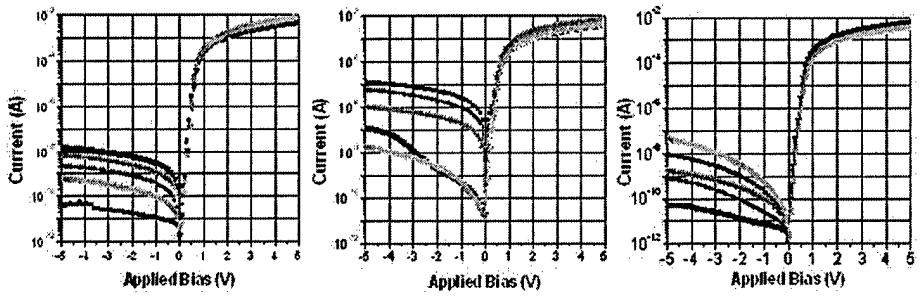

Figure 10. I-V curves for the samples in Fig. 6. From left to right are the sample contol, etched by RIE for 0.3micron, and etched for 30 seconds in KOH followed by RIE, respectively.

Table 4 shows the data collected from the MOCVD grown samples which have been investigated under different RIE etching conditions.. The as-grown sample has the 0.27 nm roughness value.

Pressure (mTorr)	Power(W)	Etch Rate (nm/Min)	Roughness RMS(nm)
60	100	2.1	0.88
	200	6.7	1.34
	300	38.5	0.54
	400	67	5.82
80	100	2.4	1.19
	200	6.0	0.55
	300	27	5.53
	400	59.8	1.86

Table 4. Etch rate with increasing pressure and power.

These results indicate that the etch rate increases with increasing RF power and the etch rate decrease slightly with increase of the reactor pressure. Increase pressure leads to reduce relatively high ionic content in the plasma which causes a reduction in the etch rate. Howevefr, there is no clear relationship between power and pressure, and roughness. What is clear is that the surface is rougher after etching. The etch rate for different pressures and PL spectra of GaN samples are shown in Figure 9 after RIE etching for different plasma power levels along with the control sample. We can see that the PL intensity decreased after etching, specifically with increasing power. Decrease in the luminescence efficiency could be understood considering the following reaction paths for removal of GaN from the surface.

$$2GaN \rightarrow N_2 + 2Ga \text{ or } GaN + N \rightarrow N_2 + Ga$$

It can be seen that the deficiency of N element (N vacancies) causes point defect on the surface. In short the PL measurement indicates a decrease in the crystal quality which is consistent with the literature.

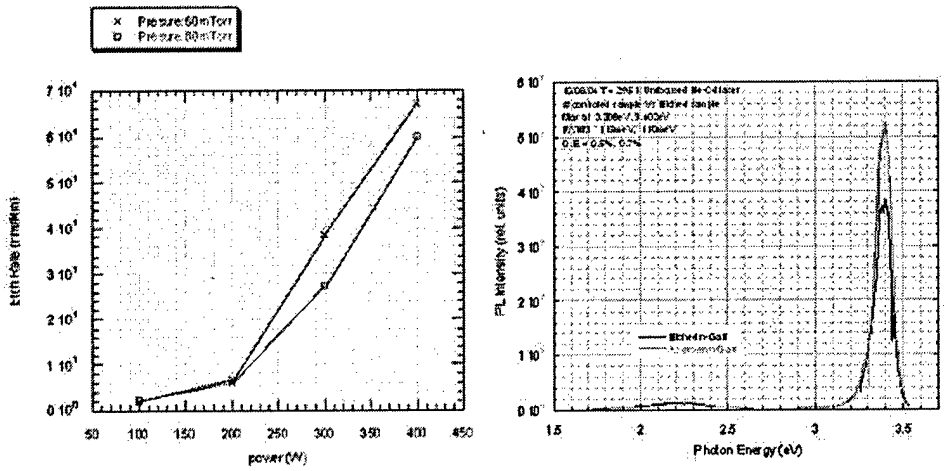

Figure 11. The etch rate at different pressures (left) and PL spectra of GaN samples (right) after RIE etching under different plasma power levels together with the control sample

The RIE etching experiment, starting with higher power ending with lower power, has also been carried out in order to determine whether the damages caused by RIE could be removed from the surface and investigate the effects of etching on metal-semiconductor interfaces and surface states. For this purpose, a control sample (CVD 287), and five different etching conditions have been investigated as tabulated in Table 5.

Name	Etch Condition	Roughness (nm)	Band Bending(V)
Etch20	300W/200W, 3min+3min	2.589	1.69
Etch21	300W/150W, 3min+3min	2.513	1.74
Etch22	300W/100W, 3min+3min	0.629	1.61
Etch23	300W/50W, 3min+3min	1.692	1.75
Etch24	300W/300, 3min+3min	6.475	1.92

Table 5. The plasma power and etching time versus roughness and band bending for different etching conditions.

As expected the 300 W, 3min+3min etch resulted in the largest roughness value and the roughness decreased with decreasing power to some extent and increased again after etching under 300W/100W etching conditions, shown in Figure 10. This shows that the best condition appears to be 300W/100W. This is a direct indication that the RIE damage caused at high power levels can be at least partially removed followed by subsequent lower power RIE etch. When the power level was decreased further, the low power could not remove the damage caused by high power RIE.

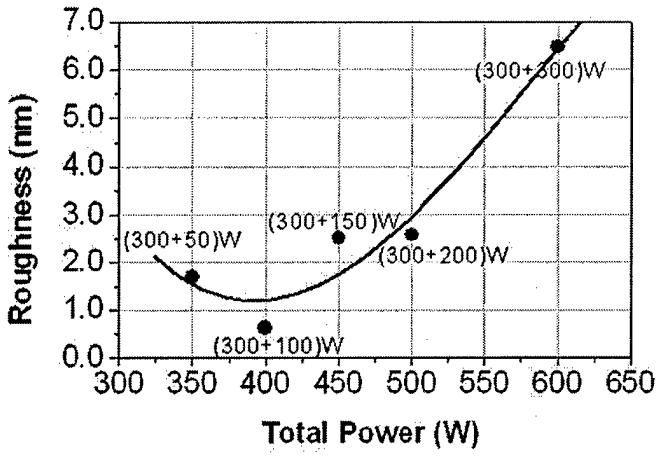

Figure 12. The variation of the roughness with total RIE plasma power.

Publications:

1. M. A. Reshchikov, D. Huang, L. He, P. Visconti, J. Jasinski, Z. Liliental-Weber, and H. Morkoç, "Photoluminescence from structural defects in GaN", International conference on Defects in Semiconductors, 22 Denmark 2003, and *Elsevier. Physica B, vol.340-342, pp.440-3, 31 Dec. 2003.*

2. M. A. Reshchikov, S. S. Park, K. Y. Lee, D. Tsvetkov, V. Dmitriev, and H. Morkoç, "Persistent photoluminescence in high-purity GaN" International conference on Defects in Semiconductors, 22 Denmark 2003, and *Elsevier. Physica B, vol.340-342, pp.444-7, 31 Dec. 2003,*

3. M. A. Reshchikov, S. S. Park, K. Y. Lee, and H. Morkoç, "Unusual properties of the dominant acceptor in freestanding GaN", International conference on Defects in Semiconductors, 22 Denmark 2003, and *Elsevier. Physica B, vol.340-342, pp.448-51,31 Dec. 2003,*

4. Pouya Valizadeh, Egor Alekseev, Dimitris Pavlidis, Feng Yun, and Hadis Morkoç, "Enhancement-Mode $Al_xGa_{1-x}N$/GaN Modulation Doped Field Effect Transistors", Workshop on Compound Semiconductor Devices and Integrated Circuits, WOCSDICE-2003

5. Z. Liliental-Weber, D. Zakharov, J. Jasinski, M.A. O'Keefe and H. Morkoç "Screw dislocations in GaN grown by different methods", Microsc. Microanal. Vol. 10, pp. 47-54 (2004).

6. A. A. Pomarico, D. Huang, J. Dickinson, A. A. Baski, R. Cingolani, H. Morkoç and R. Molnar, "Current Mapping of GaN films by Conductive Atomic Force Microscopy" AVS Fall 2003 meeting

7. Xing Gu, Faxian Xiu, Shariar Sabuktagin, Ali Teke, Daniel Johnstone, Hadis Morkoç, Bill Nemeth, and Jeff Nause, "Effect of thermal treatment on ZnO substrate for epitaxial growth", Journal of Material Science: Materials in Electronics (JMS MEL), in press.

8. Michael A. Reshchikov, Ali Teke, Herbert-Paul Maruska, David W. Hill, and Hadis Morkoç, "Photoluminescence from freestanding GaN with (10$\underline{1}$0) orientation", presented at the 2003 Fall MRS meeting, Boston MA Nov. – Dec 2003

9. M. A. Reshchikov, J. Jasinski, Z. Liliental-Weber, and H. Morkoç, "Manifestation of structural defects in photoluminescence from GaN", presented at the 2003 Fall MRS meeting, Boston MA, Nov. – Dec 2003

10. S. Sabuktagin, M. A. Reshchikov, D.K.Johnstone and H. Morkoç, "Band bending near the surface in GaN as detected by a charge sensitive probe" presented at the 2003 Fall MRS meeting, Boston MA Nov. – Dec 2003, Mat. Res. Soc. Symp. Proc. **798**, Y5.39 (2004).

11. X. Gu, F. Xiu, M. A. Reshchikov, L. He, F. Yun, D.Johnstone, J. Nause, and H. Morkoç, "high optical efficiencyGaN layers on O and Zn face ZnO" presented at the 2003 Fall MRS meeting, Boston MA Nov. – Dec 2003

12. L. He, M. A. Reshchikov, J. Spradlin, J. Xie, F. Xiu, X. Gu, F. Yun, A. A. Baski, and H. Morkoç, "GaN layers regrown on etched GaN templates by plasma assisted molecular beam epitaxy", presented at the 2003 Fall MRS meeting, Boston MA Nov. – Dec 2003

13. Hadis Morkoç, Arup Neogi, Martin Kuball, "Growth, Structure, and optical properties of III-Nitride quantum dots" Materials Research Society Fall 2003 meeting, Boston MA Dec 2003, in Progress in Compound Semiconductor Materials III – Electronic and Optoelectronic Applications, Ed. D. J. Friedman, O. Manasreh, I.A. Buyanova, A. Munkholm, and F. D. Auret, Vol. 799, pp. 325-343, 2004.

14. Arup Neogi, B. Gorman, and Hadis Morkoç, "Silver nanoparticle induced modification of spontaneous emission in GaN quantum dots", Materials Research Society Fall 2003 meeting, Boston MA Dec 2003

15. Ashutosh Sagar, R. M. Feenstra, T. S.Kuan, F. Yun, and Hadis Morkoç, "Dislocation Propagation and Strain Relaxation in GaN Films on Porous SiC" Materials Research Society Fall 2003 meeting, Boston MA Dec 2003

16. Ali Teke and Hadis Morkoç, "III-Nitrides", in Handbook of Electronic Materials, Ed. Salah Kasap and Peter Capper, Kluwer Academic Publishers, in press.

17. D. Huang, Y. Fu, and H. Morkoç, "Preparation, and Structural and Optical Properties of GaN based quantum dots", Ed. T. Steiner, Artech House

18. L. He, M. A. Reshchikov, X. Gu, F. Yun, A. A. Baski, and H. Morkoç, "GaN Layers Re-grown on GaN Templates with Nano-pits by Plasma Assisted Molecular Beam Epitaxy", International Symposium on Clusters and Nano-Assemblies (ISCANA), Oct. 2003 Richmond VA.

19. J. Spradlin, S. Dogan, J. Xie, A.A. Pomarico, R. Molnar, A.A. Baski, H. Morkoç, "Local Current Conduction of GaN Films studied by C-AFM", International Symposium on Clusters and Nano-Assemblies (ISCANA), Oct. 2003 Richmond VA.

20. J. Spradlin, S. Dogan, J. Xie, A.A. Pomarico, R. Molnar, A.A. Baski, H. Morkoç, "Conductive AFM studies of GaN Films", 8th Wide bandgap nitride workshop, September 29- October 2, 2003, Richmond, VA

21. Sang-Jun Cho, Seydi Doğan, Shahriar Sabuktagin, Michael A. Reshchikov, Daniel K. Johnstone, and Hadis Morkoç, "Study of Plasma-Induced Damage in GaN using Photoluminescence and Electron-Force Microscopy", 8th Wide bandgap nitride workshop, September 29- October 2, 2003, Richmond, VA

22. S. K. Zhang, W. B. Wang, R. R. Alfano, Teke, M. Reshchikov, L. He, S. Dogan, F. Yun and H. Morkoç, "Photionization cross-sections of deep centers in GaN/AlGaN MQW detectors", 8th Wide bandgap nitride workshop, September 29- October 2, 2003, Richmond, VA

23. Xing Gu, Faxian Xiu, Shariar Sabuktagin, Ali Teke, Daniel Johnstone, Hadis Morkoç, Bill Nemeth, and Jeff Nause, "Effect of thermal treatment on ZnO substrate for epitaxial growth", 8th Wide bandgap nitride workshop, September 29- October 2, 2003, Richmond, VA

24. C.Liu, Ali Teke Ümit Özgür, and H. Morkoç "RF sputtering deposition of high quality ZnO thin films" Wide bandgap nitride workshop, September 29- October 2, 2003, Richmond, VA

25. Charlie Fulton, R. Nemanich, R. F. Davis, C.Liu, Sang-Jun Cho, and H. Morkoç, "Band discontunities at a GaN/ZnO interface", 8th Wide bandgap nitride workshop, September 29- October 2, 2003, Richmond, VA

26. M. A. Reshchikov, S. S. Park, K. Y. Lee, B. Nemeth, J. Nause, X. Gu, and H. Morkoç, Persistent photoluminescence in high-purity GaN and ZnO", 8th Wide bandgap nitride workshop, September 29- October 2, 2003, Richmond, VA

27. L. He, M. A. Reshchikov, X. Gu, F. Yun, A. A. Baski, and H. Morkoç, "GaN layers re-grown on etched GaN templates by plasma assisted molecular beam epitaxy", 8th Wide bandgap nitride workshop, September 29- October 2, 2003, Richmond, VA

28. K. S. Ramaiah, M. A. Reshchikov, A. Teke*, L. He, F. Yun, and H. Morkoç, "Characterization of $Al_xGa_{1-x}N$/GaN Quantum Wells Grown under Ga-rich and N-rich Conditions by MBE", 8th Wide bandgap nitride workshop, September 29- October 2, 2003, Richmond, VA

29. Ali Teke, Ümit Özgür, Xing Gu, Seydi Doğan, Sang-Jun Cho, Bill Nemeth, Jeff Nause, Henry O. Everitt, Daniel K. Johnstone and Hadis Morkoç, "Contineous wave and time-resolved photoluminescence measurements on bulk ZnO substrates", 8th Wide bandgap nitride workshop, September 29- October 2, 2003, Richmond, VA

30. C.-G. Stefanita, F. Yun, H. Morkoç and S. Bandyopadhyay, "Self assembled quantum structures using porous alumina on Si substrates", in Recent Research Developments in Physics, 2004

31. Sang-Jun Cho, Seydi Dogan, Shahriar Sabuktagin, Michael A. Reshchikov, Daniel K. Johnstone, and Hadis Morkoç, "Surface band bending in as grown and plasma treated n-type GaN films using surface potential electric force microscopy", Appl. Phys. Letts, **84**, 3070 (2004).

32. Xing Gu, Ali Teke, Daniel Johnstone, Hadis Morkoç, Bill Nemeth, and Jeff Nause, "GaN epitaxy on thermally treated c-plane bulk ZnO substrates with O and Zn faces", Appl. Phys. Letts, vol.84, no.13, pp.2268-2270, 29 March 2004.

33. J. Spradlin, S. Dogan, J. Xie, R. J. Molnar, A.A. Baski, H. Morkoç, "Investigation of forward and reverse current conduction in MBE-grown GaN films by conductive atomic force microscopy", Appl. Phys. Letts, vol.84, no.21, pp.4150-4152, 24 May 2004.

34. A. Teke, Ü. Özgür, S. Doğan, X. Gu, H. Morkoç, Bill Nemeth and Jeff Nause, and Henry O. Everitt, "Excitonic Fine Structure and Recombination Dynamics in Single Crystalline ZnO", Phy. Rev. B, pending, MDA, AFOSR, and ONR.

35. Y.M. Liu, M.Z. Kauser, M.I. Nathan, P.P. Ruden, and H. Morkoc Effects of hydrostatic and uniaxial stress on Schottky barrier heights of Ga – polarity and N – polarity n – GaN, Appl.Phys. Lett., March 22, 2004,

36. Ü. Özgür, A. Teke, C. Liu, S.-J. Cho, H. Morkoç, and H. O. Everitt, "Stimulated emission and time-resolved photoluminescence in RF-sputtered ZnO thin films", Appl. Phys. Letts, vol.84, no.17, pp.3223-2325, 26 April 2004.

37. S. K. Zhang, W. B. Wang R. R. Alfano, and H. Morkoç, "Unusual Transient Photocapacitance in GaN/AlGaN Multi-quantum Wells", Superlattices and Microstructures, Vol. 35, pp.77-84, (2004).

38. M. A. Reshchikov, S. Sabuktagin, D. K. Johnstone, and H. Morkoç, "Transient photovoltage in GaN as measured by atomic force microscope tip", J. Appl.Phys., in press.

39. S. K. Zhang, W. B. Wang, R. R. Alfano, A. Teke, L. He, S. Dogan, F. Yun, D. J. Johnstone and H. Morkoç, "Photoionization Cross Sections of Deep Centers in GaN/AlGaN Multiple Quantum Wells", Appl. Phys. Letts, pending.

40. M. A. Reshchikov, S. Sabuktagin, D. K. Johnstone, A. A. Baski, H. Morkoç, D. Tsvetkov and V. Dmitriev, "Transient photovoltage in GaN", International Workshop on Nitride Semiconductors, Pittsburgh USA, 2004, and Phys. stat. sol. in press.

41. M. A. Reshchikov and H. Morkoç, "Origin of unstable photoluminescence in GaN: bulk metastable defects or surface states?", International Workshop on Nitride Semiconductors, Pittsburgh USA 2004, and Phys. stat. sol. in press.

42. M. A. Reshchikov, J. Xie, L. He, X. Gu, Y. T. Moon, Y. Fu, J. Xu, and H. Morkoç, "Effect of Potential Fluctuations on Photoluminescence in Mg-doped GaN", International Workshop on Nitride Semiconductors, Pittsburgh USA 2004, and Phys. stat. sol. in press.

43. Ashutosh Sagar, R. M. Feenstra, C. K. Inoki, T. S. Kuan, Yi Fu, Y. T. Moon, Hadis Morkoç, "Dislocation density reduction in GaN by *in situ* deposition of SiN interlayers", International Workshop on Nitride Semiconductors, Pittsburgh USA 2004, and Phys. stat. sol. in press.

44. D. Johnstone, S. Dogan, Y. T. Moon, Y. Fu, J. Xu, F. Yun, J. Leach, and H. Morkoç, "Deep Level Transient Spectroscopy of KOH Etched and MOCVD Regrown GaN" International Workshop on Nitride Semiconductors, Pittsburgh USA 2004, and Phys. stat. sol. in press.

45. F. Yun, S. Dogan, Y. T. Moon, Y. Fu, D. Johnstone, and H. Morkoç, "Characterization of MOCVD Grown GaN on Porous SiC Templates", International Workshop on Nitride Semiconductors, Pittsburgh USA 2004, and Phys. stat. sol. in press.

46. F. Yun, Y. Fu, Y. T. Moon, Ü. Özgür, J.Q. Xie S. Dogan, , and H. Morkoç, C. K. Inoki, T. S.Kuan, L. Zhou, and D. J. Smith, and," Reduction of Threading Dislocations in GaN Overgrowth by MOCVD on TiN Nanoporous Network Templates", International Workshop on Nitride Semiconductors, Pittsburgh USA 2004, and Phys. stat. sol. in press.

47. Y. T. Moon, Y. Fu, F. Yun, M. Mikkelson, D. Johnstone, and H. Morkoç, "A Study of GaN Regrowth on the Micro-Facetted GaN Template Formed by In-Situ Thermal Etching", International Workshop on Nitride Semiconductors, Pittsburgh USA 2004, and Phys. stat. sol. in press.

48. H. Morkoç, "A View of Nanoscale Electronic Devices", Workshop on Compound Semiconductor Devices and Integrated Circuits, INVITED, May 16-19, 2004 Bratislava, Slovakia

49. S. Doğan, D. Johnstone, F. Yun, S. Sabuktagin, A. A. Baki, H. Morkoç, G. Li, and B. Ganguly, "The effect of hydrogen etching on 6H-SiC studied by temperature dependent current-voltage and atomic force microscopy", Appl. Phys. Lett., pending

50. D. Johnstone, S. Dogan, Y. Moon, M. Reshchikov, F. Yun, J. Leach, Yi Fu, Y. Hu, and H. Morkoç, "Reduction of point defects in GaN by KOH etching and MOCVD overlayer regrowth", APL to be submitted.

51. Arup Neogi, Henry Everitt, Hadis Morkoç, and Atsushi Takeuchi, "Size Dependence of Carrier Recombination Efficiency in GaN Quantum Dots", IEEE Transactions of nanotechnology, in press.

52. Michael A. Reshchikov, and Hadis Morkoç, "Defects in GaN", J of Appl. Phys. Rev. in press

53. A. Teke, et al. J. Appl Phys. Reviews, Review of ZnO, submitted

54. Hadis Morkoç, "A View of Nanoscale Electronic Devices", Workshop on Compound Semiconductor Devices and Integrated Circuits, Bratislava. Slovakia, 17-19 May 2004.

55. Arup Neogi, Purnima B. Neogi, Abhijit Sarkar, and Hadis Morkoç "Self-assembled DNA molecules conjugated to GaN semiconductor nanostructures for radiative decay engineering", Presented at CLEO/IQEC San Francisco, CA May 16-21, 2004.

56. M. A. Reshchikov, D. Huang, L. He, H. Morkoç, J. Jasinski and Z. Liliental-Weber
S. S. Park and K. Y. Lee, "Manifestation of edge dislocations in photoluminescence of GaN", Appl. Phys. Lett. Pending.

D. Johnstone, S. Dogan, J. Leach, Y.T. Moon, and H. Morkoç, "Thermal stability of electron traps in GaN grown by metal-organic chemical vapor deposition", Applied Physics Letters, Nov. 8, 2004

57. Yi Fu, F. Yun, Y. T. Moon, J. Q. Xie, Ü. Özgur, S. Dogan, H. Morkoç, T. S. Kuan, C. K. Inoki, L. Zhou and D. J. Smith, "Reduction of Threading Dislocations in GaN Overgrowth by OMVPE on TiN Micro-Porous Network Templates", Appl. Phys. Lett. Pending.

58. C. Liu, F. Yun, Pierre Ruterana, Sang-Jun Cho, B. Xiao, H. Morkoç, "Structural analysis of Mn-doped ZnO thin films deposited by RF magnetron sputtering" Fall MRS 04

59. Ya.I.Alivov, M.A.Reshchikov, S.Dogan, D.C.Look, V.I. Zinenko, Yu.A. Agafonov, B.M. Ataev, V.V. Mamedov, and H.Morkoç, "Blue-violet emission from N^+ implanted ZnO:Ga films grown by chemical vapor deposition" Fall MRS 04

60. M. A. Reshchikov and H. Morkoç, "Unusual properties of the red and green luminescence bands in Ga-rich GaN", Fall MRS 04

61. M. A. Reshchikov, L. He, R. J. Molnar, S. S. Park, K. Y. Lee, and H. Morkoç, "Aquamarine luminescence band in undoped GaN", Fall MRS 04

62. C.C. Fulton, R.J. Nemanich, C. Liu, Sang-Jun Cho, H. Morkoç, "Heterojunction band offset measurements of the ZnO-GaN interface", Fall MRS 04

63. Arup Neogi, Jianyou Li, Harsheetal Liddar, Padmarekha Vemuri, Brian P. Gorman Terry Golding, Purnima B. Neogi, Abhijit Sarkar, and Hadis Morkoç, "Self-assembled olegonucleotide semiconductor conjugated to GaN nanostructures for biophotonic applications", Fall MRS 04

64. F. Yun, J. Nause, Varatharajan Rengarajan, and H. Morkoç, "Magnetic Properties of Epitaxially Grown $Zn_{1-x}Co_xO$ Thin Films", Fall MRS 04

65. Xing Gu, Seydi Dogan, Tacettin Yildirim, Daniel Johnstone, Jeff Nause, Bill Nemeth, Cole W. Litton, and Hadis Morkoç, "Electrical characterization of AlGaN/GaN MODFET on bulk ZnO substrate", 3rd international ZnO Workshop, Oct 5-8, 2004, Sendai Japan.

66. Ya. I. Alivov, E. Kalinina, S. Dogan, Ü. Özgür, C. Liu, T. Yildirim, Y. Hu, B. Xiao, Y. Zhang, and H. Morkoç, "Properties of p-SiC/n-ZnO Heterostructures Grown by Plasma-Assisted Molecular Beam Epitaxy", 3rd international ZnO Workshop, Oct 5-8, 2004, Sendai Japan.

67. Y. I. Alivov, S. Dogan, C. Liu, Ü. Özgür, Y. Moon, S. Cho, G. Xing, Y. Zhang, B. Xiao, and H. Morkoç, "Growth of p-GaN/n-ZnO/n-GaN Double Heterostructures", 3rd international ZnO Workshop, Oct 5-8, 2004, Sendai Japan.

68. Varatharajan Rengarjan, Feng Yun, Jeff Nause, and Hadis Morkoç, "Epitaxial Growth and Room Temperature Ferromagnetism in Co Doped ZnO Thin Films", 3rd international ZnO Workshop, Oct 5-8, 2004, Sendai Japan.

69. Arup Neogi, Hadis Morkoç, Takamasa Kuroda and Atsushi Tackeuchi, "Coupling of spontaneous emission from GaN/AlN quantum dots into silver surface plasmons", Optics Letters, 2004 in press.

70. Arup Neogi, Abhijit Sarkar, Jianyou Li, Purnima Neogi, and Hadis Morkoç, "Self-assembled modified deoxyguanosines conjugated to GaN quantum dots for biophotonic applications", Electronics letters, 2004 in press.

71. Arup Neogi and Hadis Morkoç, "Resonant Surface plasmon-induced modification of photoluminescence from GaN/AlN quantum dots" Institute of Physics, Nanotechnology Vol. **15,** pp.1252–1255 (2004).

72. Arup Neogi, Brian P. Gorman, Hadis Morkoç, Tadashi Kawazoe, Motoichi Ohtsu, "Near-field Optical Spectroscopy and Microscopy of Self-assembled GaN/AlN nanostructures" Optics letters, in press.

73. A. Neogi, H. Morkoç, T. Kuroda, A. Tackeuchi, T. Kawazoe, and M. Ohtsu, "Exciton localization in vertically coupled GaN/AlN quantum dots", Appl. Phys. Letts. in press

74. Arup Neogi, Hadis Morkoç, Tadashi Kawazoe, Motoichi Ohtsu, and Atsushi Tackeuchi, "Exciton dynamics in laterally coupled GaN/AlN quantum dots", PRL pending

References:

[1] Y. Oshima, T. Eri, M. Shibata, H. Sunakawa, and A. Usui, Phys. Stat. Sol. (a) 194, No. 2, 554 (2002).

[2] F. Yun, M. A. Reshchikov, K. Jones, P. Visconti, H. Morkoç, S. S. Park, and K. Y. Lee, Solid-State Elect. **44**, 2225 (2000).

[3] H. Miyake, M. Yamaguchi, T. Maeda, and I. Akasaki, MRS Internet J. Nitride Semicond. Res. **551**, W2.3 (2000).

[4] T. Wosinski, J. Appl. Phys., 65(4), 1566 (1989).

[5] L. Wu, W. E. Meyer, F. D. Auret, M. Hayes, Physica B **340-342**, 475-478 (2003).

[6] D. Johnstone S. Doğan, J. Leach, Y.T. Moon, Y. Fu, Y. Hu, and H. Morkoç, "in publication, Accepted in Appl. Phys. Lett

[7] H. Morkoç, "Nitride semiconductors and devices", Sringer, Berlin, 1999

[2] S. Nakamura, T. Mukai, and M. Senoh, Appl. Phys. Lett. **64**, 1687 (1994).

[9] S. Nakamura, M. Senoh, S. Nakahama, N. Iwasa, T. Yamada, T. Matsushita, S. Sukimoto, and Kiyoku, Appl. Phys. Lett. **70**, 616 (1997).

[10] M. Razeghi and A. Rogalski, J. Appl. Phys. **79**, 7433 (1996).

[11] Hadis Morkoç, Aldo Di Carlo and R. Cingolani, Solid State Electronics, **46**, 157 (2002).

[12] E. J. Tarsa, B. Heying, X. H. Wu, P. Fini, S. P. DenBaars, and J. S. Speck, J. Appl. Phys. **82**, 5472 (1997).

[13] F. Widmann, B. Daudin, G. Feuillet, N. Pelekanos, and J. L. Rouviere, Appl. Phys. Lett. **73**, 2642 (1998).

[14] B. Heying, E.J. Tarsa, C. R. Elsass, P. Fini, S.P. DenBaars, and J. S. Speck, J Appl. Phys. **85**, 6470 (1990).

[15] R. Held, Be. E. Ishaug, A. Parkhomovsky, A. M. Dabiran, and P. I. Cohen, J. Appl. Phys. **87**, 1219 (2000).

[16] C. Adelmann, J. Brault, D. Jalabert, P. Gentile, H. Mariette, G. Mula, and B. Daudin, J. Apply. Phys. **91**, 9638 (2002).

[17] C. Adelmann, J. Brault, G. Mula, and B. Daudin, Phys. Rev. B, **67** 165419 (2003).

[18] S. Guha, N. A. Bojarczuk, and D. W. Kisker, Appl. Phys. Lett. **69**, 2879 (1996).

[19] Gregor Koblmuller, Robert Averbeck, Henning Tiechert and Peter Pongratz, Phys. Rev. B, **69**, 035325 (2004)

[20] N. Grandjean, J. Massies, F. Semond, S. Yu. Karpov, and R. A. Talalaev, Appl. Phys. Lett. **74**, 1854 (1999).

[21] R. P. Burns, K. A. Gabriel, and D. E. Pierce, J. Am. Ceram. Soc. **76**, 273 (1993).

[22] L. X.. Zheng, M. H. Xie, and S. Y. Tong, Phys. Rev. B, **61**, 4890 (2000).

23 J. P. Reithmajer, R. F. Broom, and H. P. Mejer, Appl. Phys. Lett. **61**, 1222 (1992)

[24] C. R. Jones, K. R. Evans, T. Lei, and R. Kaspi, Mater. Res. Soc. Symp. Proc. (1), 0 (1996).

[25] P. Hacke, G. Feuillet, H. Okumura, and S. Yoshida, Appl. Phys. Lett. **69** 2507 (1996).

[26] Charles Kittel, "Introduction to solid state physics", John Wiley& Sons, New York (1971).

[27] J. M. Myoung, O. Gluschenkov, K. Kim, and S. Kim, J. Vac. Sci. Technol. A **17**, 3019 (1999).

[28] A. R. Smith, R. M. Feenstra, D. W. Greve, M. S. Shin, M. Skowronski, J. Neugebauer and J. E. Northrup, J. Vac. Sci. Technol. B **16**, 2242 (1998).

[29] Oliver Brandt, Yue Jun Sun, Lutz Daweritz, and Klaus H. Ploog, Phys. Rev. B **69** 165326 (2004).

[30] John E. Northrup, J. Neugebauer, R. M. Feenstra, A. R. Smith, Phys. Rev. B, **61**, 9932 (2000).

[31] A. R. Smith R. M. Feenstra, D. W. Greve, J. Neugebauer, and J. E. Northrup, Phys. Rev. Lett. **79,** 3934 (1997).

[32] Tosja Zywietz, Jorg Neugebauer, and Matthias Scheffler, Appl. Phys. Lett. **73**, 487 (1998).

[33] H. Liu, J. G. Kim, M. H. Ludwig, and R. M. Park, Appl. Phys. Lett. **71**, 347 (1997).